UNIVERSITY OF AMSTERDAM

UvA-DARE (Digital Academic Repository)

Infrared spectra of protonated polycyclic aromatic hydrocarbon molecules: Azulene

Zhao, D.; Langer, J.; Oomens, J.; Dopfer, O.

DOI
10.1063/1.3262720

Publication date
2009

Document Version
Final published version

Published in
Journal of Chemical Physics

Link to publication

Citation for published version (APA):
Zhao, D., Langer, J., Oomens, J., & Dopfer, O. (2009). Infrared spectra of protonated polycyclic aromatic hydrocarbon molecules: Azulene. *Journal of Chemical Physics*, *131*(18), 184307. https://doi.org/10.1063/1.3262720

General rights
It is not permitted to download or to forward/distribute the text or part of it without the consent of the author(s) and/or copyright holder(s), other than for strictly personal, individual use, unless the work is under an open content license (like Creative Commons).

Disclaimer/Complaints regulations
If you believe that digital publication of certain material infringes any of your rights or (privacy) interests, please let the Library know, stating your reasons. In case of a legitimate complaint, the Library will make the material inaccessible and/or remove it from the website. Please Ask the Library: https://uba.uva.nl/en/contact, or a letter to: Library of the University of Amsterdam, Secretariat, Singel 425, 1012 WP Amsterdam, The Netherlands. You will be contacted as soon as possible.

UvA-DARE is a service provided by the library of the University of Amsterdam (https://dare.uva.nl)

Download date:09 Mar 2023

Infrared spectra of protonated polycyclic aromatic hydrocarbon molecules: Azulene

Dawei Zhao,[1] Judith Langer,[1] Jos Oomens,[2] and Otto Dopfer[1,a)]
[1]*Institut für Optik und Atomare Physik, Technische Universität Berlin, Hardenbergstrasse 36, Berlin D-10623, Germany*
[2]*FOM Institute for Plasma Physics, Rijnhuizen, P.O. Box 1207, Nieuwegein 3430BE, The Netherlands and University of Amsterdam, Nieuwe Achtergracht 166, Amsterdam 1018WV, The Netherlands*

(Received 24 August 2009; accepted 20 October 2009; published online 13 November 2009)

The infrared (IR) spectrum of protonated azulene ($AzuH^+$, $C_{10}H_9^+$) has been measured in the fingerprint range (600–1800 cm^{-1}) by means of IR multiple photon dissociation (IRMPD) spectroscopy in a Fourier transform ion cyclotron resonance mass spectrometer equipped with an electrospray ionization source using a free electron laser. The potential energy surface of $AzuH^+$ has been characterized at the B3LYP/6-311G** level in order to determine the global and local minima and the corresponding transition states for interconversion. The energies of the local and global minima, the dissociation energies for the lowest-energy fragmentation pathways, and the proton affinity have been evaluated at the CBS-QB3 level. Comparison with calculated linear IR absorption spectra supports the assignment of the IRMPD spectrum to C4-protonated $AzuH^+$, the most stable of the six distinguishable C-protonated $AzuH^+$ isomers. Comparison between Azu and C4-$AzuH^+$ reveals the effects of protonation on the geometry, vibrational properties, and the charge distribution of these fundamental aromatic molecules. Calculations at the MP2 level indicate that this technique is not suitable to predict reliable IR spectra for this type of carbocations even for relatively large basis sets. The IRMPD spectrum of protonated azulene is compared to that of isomeric protonated naphthalene and to an astronomical spectrum of the unidentified IR emission bands. © *2009 American Institute of Physics*. [doi:10.1063/1.3262720]

I. INTRODUCTION

The protonation of aromatic molecules is a central process in biology and organic chemistry. Protonated aromatic molecules, denoted AH^+, are frequently invoked as reactive intermediates in fundamental organic ionic reaction mechanisms.[1] For example, they are widely accepted to occur as transient σ complexes in electrophilic aromatic substitution, the most important reaction class of aromatic molecules.[1,2] It is well recognized that fundamental properties of ion-molecule reactions, such as energetics and dynamics, sensitively depend on the solvation environment, because of the strong interaction between the charge of the reacting ionic species and the surrounding solvent molecules. The detailed understanding of the impact of solvation on the properties of such ion-molecule reaction mechanisms requires the characterization of AH^+ ions under isolated and controlled microsolvation conditions. Other fundamental fields, in which AH^+ plays a crucial role, are combustion,[3] interstellar chemistry (*vide infra*),[4–6] and biochemistry.[7,8]

Until recently, experimental information about isolated AH^+ ions was almost exclusively based on mass spectrometry,[9] which provides only indirect and often ambiguous structural information. Spectroscopic information to determine, for example, directly the preferred protonation sites in isolated AH^+ ions have been lacking because of the difficulties encountered in the production of sufficient ion concentrations. The notable exception has been the pioneering work by Beauchamp and Freiser, who obtained low-resolution electronic photodissociation spectra of a variety of AH^+ ions.[10] However, these spectra were broad and unstructured and did not provide any information about the geometry of the AH^+ ions, in particular about the protonation site. Recent progress in the development of sensitive infrared (IR) photodissociation (IRPD) schemes allowed for the first time to spectroscopically characterize isolated[11] and microsolvated[12] AH^+ ions in the gas phase.

Two major IR photodissociation strategies have successfully been applied to AH^+ ions as has been reviewed recently.[13] The first technique employs modern, relatively low-intensity, optical parametric oscillator laser systems in the frequency range 800–4000 cm^{-1} to drive one-photon IRPD of AH^+-L_n cluster ions.[12] This approach is based on the evaporation of one or more of the weakly bound ligands upon resonant absorption of a single photon (messenger technique),[14] and has been applied to a variety of AH^+-L_n cluster ions, including A=benzene,[15–18] phenol,[12,19] fluorobenzene,[20] para-halogenated phenols,[21] toluene,[17] pyridine,[18] aniline,[22] imidazole,[23] various amino acids and peptides,[24] and neurotransmitters.[25] The IRPD method can also be applied to break weak chemical bonds in certain AH^+ isomers,[11,26] but usually fails to dissociate common AH^+ ions because the energy of a single IR photon is insufficient to break strong covalent bonds. This limitation is overcome by the second technique, which utilizes high-intensity IR free electron lasers (IR-FELs) in the frequency range

a)Author to whom correspondence should be addressed. Electronic mail: dopfer@physik.tu-berlin.de. Telephone: ++49 30 314 23017. Fax: ++49 30 314 23018.

 © 2009 American Institute of Physics

Downloaded 16 Apr 2010 to 145.18.109.182. Redistribution subject to AIP license or copyright; see http://jcp.aip.org/jcp/copyright.jsp

500–2500 cm^{-1} to drive IR multiple photon photodissociation (IRMPD) processes of AH^+ ions in the fingerprint range.[27] This IRMPD approach has recently been applied to a range of simple AH^+ ions with, for example, A=benzene,[27] fluorobenzene,[28] phenylsilane,[29] toluene,[30] benzaldehyde,[31] furan,[32] pyrrole,[32] indazole,[33] benzoic acid,[34] naphthalene,[35] and several DNA bases.[36] The IR(M)PD studies of isolated and microsolvated AH^+ ions mainly addressed the questions of the preferred protonation site(s), the photofragmentation behavior, and the influence of stepwise microsolvation in a polar and nonpolar environment.

The IRMPD mechanism and its effects on the appearance of the IR spectrum of a molecular ion have been discussed previously.[37,38] The sequential absorption of multiple IR photons required to dissociate the ion results, via vibrational anharmonicities, in broadening and frequency shifts of the transitions compared to those observed in linear IR absorption spectra.[17,37,38] The redshifts and widths observed in IRMPD spectra are, however, typically below 20 cm^{-1}, allowing for an assignment of the IRMPD bands by direct comparison with calculated linear IR absorption spectra. To this end, the IRMPD technique has successfully been applied to the IR spectroscopy of a broad variety of ions and ionic complexes, and the interested reader is referred to recent reviews for further details.[13,37–39]

The present work reports the IRMPD spectrum of protonated azulene, $AzuH^+$. $AzuH^+$ is an isomer of protonated naphthalene, which is the prototypical polycyclic aromatic hydrocarbon molecule (PAH). Laboratory IR and electronic spectra of isolated protonated PAH molecules, H^+PAH, are also of interest for comparison with astronomical spectra, in particular the so-called unidentified IR (UIR) emission bands observed in the 3–20 μm range[5,40] and the yet unassigned diffuse interstellar bands (DIBs) occurring in the 400–1300 nm range.[41] Although it is now widely accepted that PAH and PAH^+ are present in the interstellar medium and mainly responsible for the UIR bands,[5,6,42] H^+PAH molecules have recently also been invoked to contribute to both the UIR and the DIB spectra,[43] in particular since protonation of PAHs via rapid H-atom attachment to PAH^+ was found to be an efficient process.[4,44] To test this hypothesis, laboratory IR and electronic spectra of isolated H^+PAH molecules are required. However, these spectra are largely lacking, with the notable exception of the recently reported IR spectrum of protonated naphthalene obtained by IRMPD.[35] Significantly, the IRMPD spectrum of protonated naphthalene,[35] obtained in the fingerprint range, is rather different from that of benzene,[17,27,28] indicating that the appearance of the IR spectrum strongly depends on the number of aromatic rings (at least for small PAH size). Hence, IR spectra of larger H^+PAH are required in order to follow the evolution of the IR spectrum as a function of the PAH size. Interestingly, whereas the IR spectrum of protonated benzene differs considerably from the UIR spectrum,[16,35] the IRMPD spectrum of protonated naphthalene shows striking coincidences with the UIR spectrum.[35] Therefore, we initiated a program to investigate the IR spectra of further H^+PAH molecules, and the present work reports results on $AzuH^+$. IRMPD spectra of larger H^+PAH obtained up to size of protonated coronene are compared with the UIR bands elsewhere.[45] The spectra of these larger H^+PAH ions are also of fundamental importance in light of various astrochemical models, which suggest PAH molecules consisting of 20–80 C atoms to be photochemically most stable in interstellar clouds.[5,6,46]

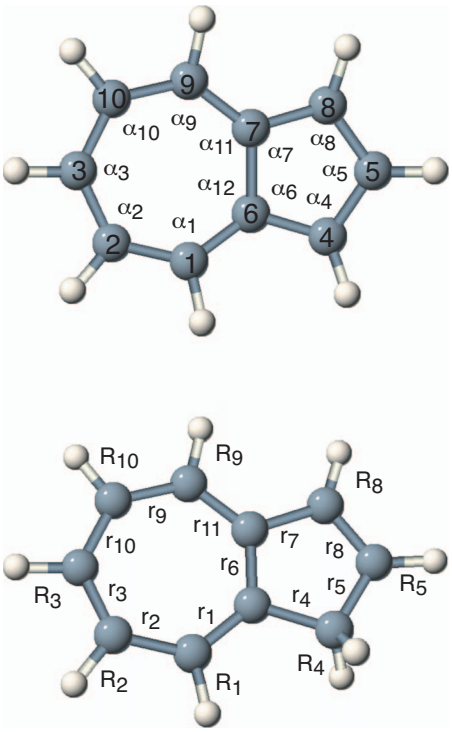

FIG. 1. Structures of azulene (C_{2v}) and the most stable isomer of protonated azulene (C4-$AzuH^+$, C_s) in their electronic ground states ($^1A_1$, $^1A'$) calculated at the B3LYP/6-311G** level. The structural parameters are listed in Table IV.

In the following, we briefly review the knowledge of neutral and protonated azulene relevant for the present work. High-level quantum chemical calculations yield a planar C_{2v} symmetric structure for Azu in its ground electronic state (Fig. 1),[47–49] in agreement with microwave,[50–52] vibrational Raman and IR,[53] and rotationally resolved electronic spectra.[54] In contrast with neutral Azu, theoretical and experimental information on $AzuH^+$ is extremely scarce.[8,55–58] The only experimental information available comes from mass spectrometry, yielding values for the proton affinity in the range between 925 and 931 kJ/mol.[8,55–58] Quantum chemical calculations[8] suggest preferred protonation at C4 (Fig. 1), although difficulties have been noted in the evaluation of precise and reliable values for the proton affinity at this site, with differences of the order of 20 kJ/mol between DFT, MP2, and experimental results.[8,58]

To the best of our knowledge, the gas-phase IR spectrum of $AzuH^+$ reported here corresponds to the first spectroscopic detection of this fundamental molecular ion (in gas and condensed phase). It provides unambiguous information about the preferred protonation site and facilitates comparison with the astronomical UIR spectrum. Accompanying quantum chemical calculations are performed for both Azu and $AzuH^+$ in order to evaluate the effects of protonation on the structure, vibrational properties, and charge distribution of the aromatic molecule. The characterization of the potential en-

Downloaded 16 Apr 2010 to 145.18.109.182. Redistribution subject to AIP license or copyright; see http://jcp.aip.org/jcp/copyright.jsp

ergy surface of $AzuH^+$ is investigated in some detail to determine the proton affinities for the various protonation sites, the corresponding barriers for interconversion between the isomers, and the low-energy dissociation channels.

II. EXPERIMENTAL AND THEORETICAL TECHNIQUES

The IRMPD spectrum of $AzuH^+$ is obtained using a Fourier transform ion cyclotron resonance (FTICR) mass spectrometer coupled to the IR beamline of the Free Electron Laser for Infrared eXperiments (FELIX) in the Netherlands.[59] $AzuH^+$ ions are generated by electrospray ionization (ESI) using a micromass Z-spray source. For this purpose, Azu is dissolved in pure methanol. To enhance the protonation efficiency, a few drops of a 1*M* solution of ammonium acetate was added. This procedure was found to be much more efficient for protonation than using formic or acetic acid, and PAHs with a proton affinity higher than that of ammonia could readily be protonated (PA=853.6 and 925.2 kJ/mol for NH_3 and Azu, respectively).[57] The ESI source operated with about 3.8 kV on the spray capillary and a 200 V cone voltage. Ions are accumulated in a hexapole trap for about 4 s prior to being injected into the ICR cell through a 1 m long octopole ion guide. $AzuH^+$ ions are then mass isolated and irradiated with 12 macropulses from FELIX at a 5 Hz repetition rate. The macropulse energy was measured to be around 45 mJ, although it leveled off at wavenumbers larger than 1400 cm^{-1}. The full width at half maximum (FWHM) bandwidth of the radiation is typically 0.5% of the central wavelength, which corresponds to 5 cm^{-1} at 10 μm (1000 cm^{-1}). The wavelength is calibrated using a grating spectrometer and is believed to be accurate to within ± 0.02 μm, corresponding to ± 0.5 and ± 8 cm^{-1} at frequencies of 500 and 2000 cm^{-1}, respectively. The step size varies between 2 and 8 cm^{-1}, depending on the laser frequency. The main fragmentation channels observed under the present experimental conditions are the loss of atomic and molecular hydrogen. After the irradiation, a standard excite/detect sequence is used to monitor parent and fragment ion intensities. The fragment yield is then calculated as the integrated intensity of the fragment ions divided by that of parent and fragment ions. At each laser frequency, three mass spectra are averaged and the resulting fragment yields are plotted as a function of photon energy to obtain an IRMPD spectrum.

Quantum chemical calculations have been performed for Azu and $AzuH^+$ using the GAUSSIAN03 package.[60] Initial test calculations have been carried out for the most stable isomer of $AzuH^+$ at the B3LYP and MP2 levels of theory in order to establish a suitable method and basis set for the structural, energetic, and vibrational characterization. These test calculations reveal that the MP2 level fails to reproduce the frequencies and relative IR intensities of the IRMPD spectrum observed, using a variety of basis sets ranging from 6-31G* to 6-311+G** (*vide infra*). In contrast, the B3LYP level nicely reproduces the experimental IR spectrum for basis sets larger than 6-311G**. On the basis of this observation, it was decided to employ the efficient CBS-QB3 technique[61] for calculating the properties of Azu and $AzuH^+$, which is found to be a convenient compromise between the efficient calculation of reliable IR spectra and the accurate determination of energies. The CBS-QB3 model obtains optimized geometries and IR spectral properties at the B3LYP/6-311G** level, whereas the energies including contributions from zero-point energy are evaluated via extrapolation to the complete basis set (CBS) limit using correlation energy contributions determined at the MP4(SDQ)/6-31+G** and CCSD(T)/6-31G* levels and further corrections. The harmonic vibrational frequencies presented in the tables and figures are determined at the B3LYP/6-311G** level and scaled by an empirical factor of 0.9679.[62] Theoretical stick spectra are convoluted with a Gaussian line profile using a width of 20 cm^{-1} (FWHM), in order to facilitate convenient comparison with the experimental IRMPD spectra. The "intrinsic reaction coordinate for maximum of energy" technique[63] has been applied for the search of transition states, and the final optimization and evaluation of isomerization barriers has been conducted at the B3LYP/6-311G** level. Charge distributions in Azu and $AzuH^+$ were determined using the natural bond orbital (NBO) analysis at the same level.

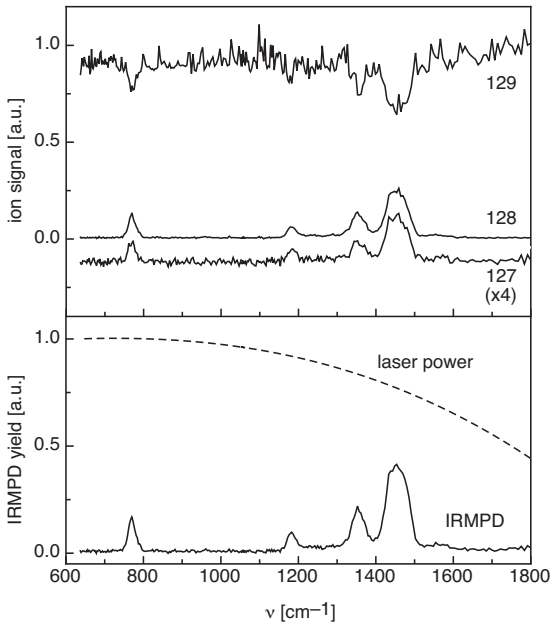

FIG. 2. Ion currents of the $AzuH^+$ parent ion (m=129 u) and the two fragment channels corresponding to the loss of H (m=128 u) and H_2 (m=127 u, multiplied by 4). Also shown is the IRMPD spectrum of $AzuH^+$ recorded in the fingerprint range (600–1800 cm^{-1}). The IRMPD yield is obtained by taking the H and H_2 loss channels into account and normalizing linearly for IR laser power (dashed line).

III. RESULTS AND DISCUSSION

A. Mass and IRMPD spectra

Two fragment channels are detected upon IR activation of $AzuH^+$ (m=129 u), namely the loss of H (m=128 u) and the loss of H_2 (m=127 u). Figure 2 shows the ion currents of the parent ion and both fragment ions as a function of the IR laser frequency. All major vibrational transitions are observed as depletion in the parent channel and as positive signal in the two fragment channels. The ratio of the signals detected in the H and H_2 loss channels is independent of the

Downloaded 16 Apr 2010 to 145.18.109.182. Redistribution subject to AIP license or copyright; see http://jcp.aip.org/jcp/copyright.jsp

TABLE I. Band maxima and widths (FWHM, in parentheses) of the transitions observed in the IRMPD spectrum of protonated azulene (Figs. 2 and 6, assignments are given in Table V).

Band	A	B	C	D	E	F	G	H	K	L	M	N
ν/cm^{-1}	770 (22)	791[a]	962 (22)	1182 (28)	1240 (~30)	1282 (20)	1325[a]	1353 (37)	1439 (25)	1461 (~50)	1555 (20)	1577 (20)

[a]Shoulder of a strong band.

laser frequency and roughly 4:1, suggesting that H loss is energetically favorable. This conclusion is supported by the calculations presented below. The depletion on the strongest resonance at ~1450 cm^{-1} amounts to roughly 30%, indicating efficient IRMPD under the present experimental conditions (~40 mJ macropulse energy). Figure 2 displays the IRMPD spectrum of $AzuH^+$ recorded in the fingerprint range (600–1800 cm^{-1}). The IRMPD yield is derived by considering both the H and the H_2 loss channels, and subsequent linear normalization for IR laser power (also shown in Fig. 2). The band maxima and widths (FWHM) of the transitions observed are listed in Table I. The linewidth of isolated transitions is of the order of 20 cm^{-1}. The observed IRMPD linewidth is a convolution of the finite laser bandwidth of 0.5% (corresponding to $\Delta\nu$=2.5–7.5 cm^{-1} for ν=500–1500 cm^{-1}), unresolved rotational structure, and spectral broadening arising from the multiple photonic character of the IRMPD process.[37,38]

B. Potential energy surface and proton affinity

Figure 3 summarizes the salient parts of the potential energy surface of $AzuH^+$ evaluated at the B3LYP/6-311G** level. Only σ complexes corresponding to protonation at the six distinguishable C atoms of azulene are considered, because π complexes of protonated aromatic molecules are saddle points on the potential.[15,64] The σ complexes are denoted Cn-$AzuH^+$, according to protonation at the C atom with number n (see Fig. 1 for the atom labeling scheme). The Cn-$AzuH^+$ minima with n=1–5 have planar aromatic molecular frameworks except for the two out-of-plane protons of the aliphatic CH_2 group, resulting in either C_s (n=1,2,4) or C_{2v} (n=3,5) symmetry. In contrast, C6-$AzuH^+$ has C_1 symmetry to satisfy tetrahedral bonding corresponding to sp^3 hybridization of the C6 atom. The relative energies of the Cn-$AzuH^+$ minima calculated at various theoretical levels are collected in Table II. The relative CBS-QB3 energies of the isomers, which are considered to be most accurate, vary in the order C4≪C2≈C5<C6<C3≈C1 (0≪94<102<121<167≈175 kJ/mol), that is C4-$AzuH^+$ is clearly by far the lowest-energy isomer. The same energetic order is obtained at the B3LYP and MP2 levels using various basis sets, ranging from 6-31G* to 6-311+G** (Table II). While the B3LYP relative energies at various basis sets are all the same to within 5 kJ/mol, they are slightly lower than the CBS-QB3 energies by 5–15 kJ/mol. Interestingly, the relative energies at the MP2/6-31G* are systematically higher than the CBS-QB3 energies by 15–30 kJ/mol. Protonation at the α-position of the five-membered ring is expected, as it implies the lowest loss in aromaticity.[65] The barriers for the 1,2 H-atom shifts of the excess proton between two neighboring minima occur at bridged transition states, in which the excess proton lies above the C–C bond and is roughly symmetrically shared between the two adjacent C atoms. These barriers are rather high for C4-$AzuH^+$ (>100 kJ/mol). Also the second most stable isomer, C2-$AzuH^+$, is trapped in a potential well of similar depth. In contrast, the isomerization barriers of the other local minima are significantly lower, suggesting more facile isomerization toward the two deep C4-$AzuH^+$ and C2-$AzuH^+$ minima.

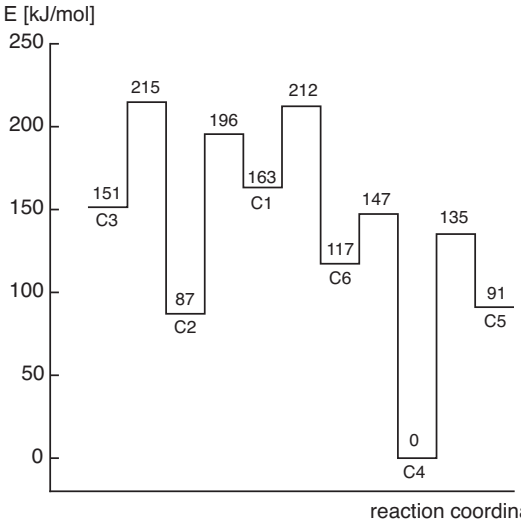

FIG. 3. Potential energy surface of $AzuH^+$ evaluated at the B3LYP/6-311G** level. The transition state for 1,2 H-atom shift from C6 to C7 lies at 227 kJ/mol.

The proton affinity for C4-$AzuH^+$ calculated at the CBS-QB3 level of 913.8 kJ/mol is lower than the experimental values of 925–931 kJ/mol by about 15 kJ/mol,[8,55–58] although the mass spectrometric experiments were not sensitive to the protonation site. Moreover, the experimental error in proton affinity determinations is typically of the order of ±10 kJ/mol. In any case, it is clear from the calculated energies for the other protonation sites that the experimental proton affinity is due to the C4-$AzuH^+$ isomer.[8] Table III compares the proton affinities obtained for this protonation site at various theoretical levels, ranging from 6-31G* to 6-311+G**. The values at the B3LYP level are systematically slightly higher than the experimental data, while those at the MP2 level show very good agreement. At the present stage, the large discrepancy between our B3LYP/6-311G** value (939 kJ/mol) and that of Ref. 8 obtained at the same level (914.2 kJ/mol) is unclear. It may arise from the fact that thermal and zero-point corrections in Ref. 8 are taken from scaled HF calculations and not directly from the B3LYP/6-311G** data as in the present work. The adiabatic ionization energy of azulene of 7.51 eV obtained at the CBS-

Downloaded 16 Apr 2010 to 145.18.109.182. Redistribution subject to AIP license or copyright; see http://jcp.aip.org/jcp/copyright.jsp

TABLE II. Relative energies (in kJ/mol) of various isomers of protonated azulene (Cn-AzuH$^+$) evaluated at several theoretical levels.

	C1-AzuH$^+$	C2-AzuH$^+$	C3-AzuH$^+$	C4-AzuH$^+$	C5-AzuH$^+$	C6-AzuH$^+$
CBS-QB3	175.0	94.1	167.0	0	102.1	120.6
B3LYP/6-311+G**	162.5	86.5	150.8	0	90.5	116.7
B3LYP/6-311G**	163.3	87.1	151.4	0	91.1	117.3
B3LYP/6-31G*	166.1	89.0	155.0	0	92.6	122.0
MP2/6-31G*	200.1	114.5	194.3	0	118.1	135.6

QB3 level agrees well with the tabulated experimental value of 7.42 eV,[66] again demonstrating the reliability of the chosen theoretical level to evaluate energies.

C. Isomer identification

Although the energetically less favorable AzuH$^+$ isomers are significantly less stable than C4-AzuH$^+$ (by more than 80 kJ/mol, Table II, Fig. 3), the barriers separating these isomers from C4-AzuH$^+$ are rather high. Thus, while thermodynamically less stable, these isomers might be formed in the ESI source and kinetically trapped in the potential well of the respective local minima due to the high isomerization barriers. If this were the case, they would be present in the AzuH$^+$ ion cloud assayed in the ICR by IRMPD. In fact, such high-lying isomers have unambiguously been detected for related protonated aromatic molecules by IRPD spectroscopy of ions generated in an electron impact cluster ion source, such as phenol,[19] para-fluorophenol,[26] and fluorobenzene.[20] For this reason, the IRMPD spectrum is compared to the IR spectra calculated for all six available AzuH$^+$ isomers in Fig. 4. Significantly, all six isomers can readily be distinguished by their rather different IR spectrum in the fingerprint range investigated. Moreover, the comparison with the experimental spectrum provides convincing evidence that the C4-AzuH$^+$ isomer is the predominant carrier of the IRMPD spectrum. Only for this isomer, rather satisfactorily agreement between the experimental and theoretical IR spectra is observed in the whole fingerprint range, with respect to both positions and intensities of the transitions. For all other isomers, the agreement is drastically worse. Thus, the comparison of the IR spectra in Fig. 4 clearly indicates that the less stable isomers provide at most a minor contribution to the observed spectrum. As a consequence of the predominant observation of the C4-AzuH$^+$ isomer, the discussion of the geometric and vibrational structure, as well as the possible dissociation pathways given below is restricted to this particular AzuH$^+$ isomer.

At this stage, it is interesting to note that vibrational spectra calculated at the MP2 level using various basis sets fail to reproduce the experimental IRMPD spectrum. Figure 5 compares IR spectra of C4-AzuH$^+$ calculated at the MP2 and B3LYP levels using a variety of basis sets, ranging from 6-31G* to cc-pVTZ. The number of basis functions (primitive Gaussians) are 168 (316), 185 (393), 234 (392), 274 (432), and 426 (683) for 6-31G*, cc-pVDZ, 6-311G**, 6-311+G**, and cc-pVTZ, respectively. Clearly, at the B3LYP level excellent agreement is observed for the 6-311G** basis set. While for smaller basis sets, the agreement is less satisfactory, the spectra for larger basis sets essentially do not change anymore. Hence, the B3LYP/6-311G** level implemented in the CBS-QB3 model chemistry has been considered as the appropriate method to obtain reliable IR spectra. In contrast, the IR spectra calculated at the MP2 level show large deviations from both the B3LYP spectra and the experimental IRMPD spectrum, indicating that it is the MP2 level that is not suitable for predicting reliable IR spectra of this type of molecules, even when using basis sets as large as 6-311+G**. This conclusion is independent of the scaling factor, which has been chosen as 0.97 for the MP2 calculations in an attempt to optimize the agreement with experiment. In fact, the recommended scaling factors for this level are much smaller (0.94–0.95),[67] which would make the disagreement between MP2 and IRMPD spectra even worse. The major discrepancy arises from the wrong prediction of the IR spectrum in the C–C stretch range (1400–1700 cm^{-1}) at the MP2 level with respect to both vibrational frequencies and IR intensities. Also, the frequency of the intense out-of-plane C–H bend in the 700–800 cm^{-1} range appears to be significantly underestimated at the MP2 level.

D. Dissociation energies

In the next step, the lowest-energy dissociation pathways of C4-AzuH$^+$ are considered. Similar to collisional activation, IRMPD involves stepwise heating via sequential ab-

TABLE III. Proton affinities (ΔH in kJ/mol at 298.15 K) of azulene for protonation at the C4 position (C4-AzuH$^+$) evaluated at several theoretical levels.

Method[a]	C4-AzuH$^+$	Reference
B3LYP/6-31G*	957.3	This work
B3LYP/6-311G**	914.2[b]	8
B3LYP/6-311G**	939.2	This work
B3LYP/6-311+G**	933.0	This work
MP2/6-31G*	935.2	This work
MP2/6-311G**	922.1	This work
CBS-QB3	913.8	This work
Experimental	930.9[c]	56
	925.2	57
	927.6	8
	928.9	55

[a]The number of basis functions (primitive Gaussians) are 168 (316), 185 (393), 234 (392), 274 (432), and 426 (683) for 6-31G*, cc-pVDZ, 6-311G**, 6-311+G**, and cc-pVTZ, respectively.
[b]Thermal and zero-point corrections evaluated at the HF level.
[c]Measured at 600 K.

Downloaded 16 Apr 2010 to 145.18.109.182. Redistribution subject to AIP license or copyright; see http://jcp.aip.org/jcp/copyright.jsp

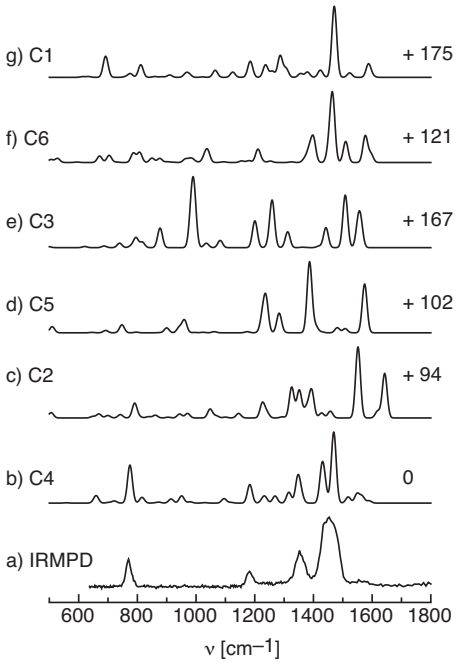

FIG. 4. IRMPD spectrum of $AzuH^+$ compared to linear IR absorption spectra of various isomers (Cn-$AzuH^+$, n=1–6) calculated at the B3LYP/6-311G** level, using a convolution width of 20 cm^{-1} (FWHM) and a scaling factor of 0.9679. Relative energies of the Cn-$AzuH^+$ isomers are given in kJ/mol (Table II).

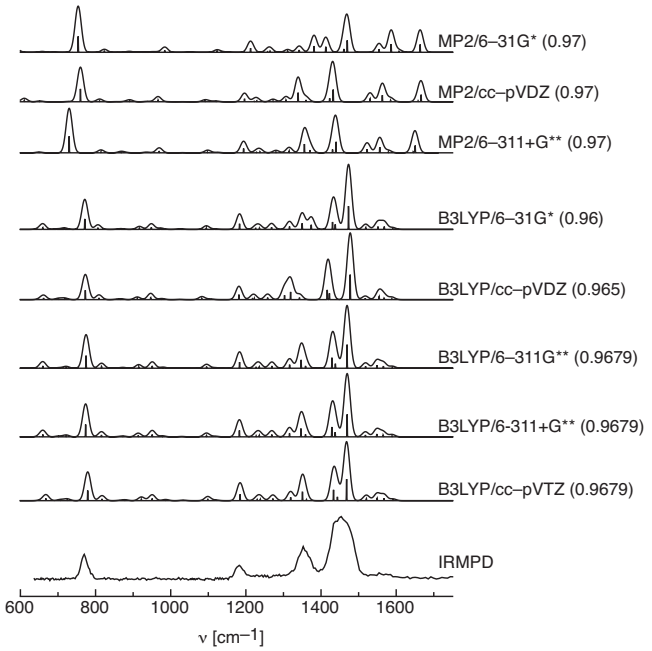

FIG. 5. Linear IR absorption spectra of the most stable isomer of protonated azulene (C4-$AzuH^+$) evaluated at the MP2 and B3LYP levels of theory compared to the IRMPD spectrum. The number of basis functions (primitive Gaussians) are 168 (316), 185 (393), 234 (392), 274 (432), and 426 (683) for 6-31G*, cc-pVDZ, 6-311G**, 6-311+G**, and cc-pVTZ, respectively. The scaling factors employed are indicated in parentheses. They are recommended values for the B3LYP level (Refs. 62 and 67) and 0.97 for the MP2 level.

sorption of multiple IR photons, eventually leading to dissociation on the ground electronic state as the dissociation threshold is reached.[37,38] As IR activation reveals only detectable signals in the H and H_2 loss channels, only the elimination of atomic and molecular hydrogen from C4-$AzuH^+$ is considered. The lowest-energy fragmentation channel corresponds to H atom loss at the C4 atom, with a dissociation energy of 326.8 kJ/mol (CBS-QB3). In analogy to isomeric protonated naphthalene, it is expected that this process occurs without barrier.[4,68] The elimination of molecular H_2 from C4-$AzuH^+$, with both H atoms coming from the C4 atom and generating $C_{10}H_7^+$ in its singlet state,[69] requires 403.6 kJ/mol, and is also expected to occur along a barrierless reverse reaction.[69,70] A similar energy of 413.4 kJ/mol is required to eliminate H_2 from C4-$AzuH^+$ with one H atom being abstracted from C4 and one from C5 in a concerted reaction. Another option for the appearance of the m=127 u channel is the abstraction of two individual H atoms, which can happen in two different ways. First, C4-$AzuH^+$ absorbs enough photons to eliminate 2 H atoms. This rather energy-demanding fragmentation is endothermic by 840.6 kJ/mol (assuming both H atoms being abstracted from C4) and thus rather unlikely to occur. The second scenario involves initial IRMPD of C4-$AzuH^+$ into the Azu^+ radical cation, which can further absorb multiple IR photons to expel the second H atom. This process is also unlikely to be observed, as the IR spectra of C4-$AzuH^+$ and Azu^+ are different so that the relative IRMPD yields observed in the m=128 and 127 u mass channels should depend on the photon energy, which is in contrast with the experimental measurement. The two H_2 loss channels considered above are significantly more energy demanding than H loss (by ~80 kJ/mol), consistent with the latter fragmentation reaction being the dominant IRMPD channel observed. Despite this large energy difference, still 20% of the IRMPD yield is detected in the H_2 loss channel. For isomeric protonated naphthalene, the difference between the dissociation energies for H and H_2 loss (260 and 290 kJ/mol)[35] is smaller than for $AzuH^+$ (30 versus 80 kJ/mol) but only 3% of the IRMPD yield was detected in the higher-energy H_2 loss channel in a comparable experiment using the IR-FEL at the Centre Laser Infrarouge d'Orsay (CLIO).[35] The branching ratios for competing fragmentation channels depend on the rates for dissociation and heating by IR activation. Hence, the observed branching ratios are sensitive to the details of the experimental IRMPD conditions (pulse sequence, duration, and energy of the FEL) and the molecular parameters (anharmonic couplings, intramolecular vibrational energy redistribution).[37] As can be seen from Fig. 2, the branching ratio for the two competing fragment channels is independent of the photon energy. Moreover, also the peak positions and widths of the resonances are the same in both channels within experimental uncertainty. This is an interesting and perhaps surprising observation[37,71] as the number of photons required for dissociation varies substantially over the spectral range investigated and the dissociation channel considered (one has to bear in mind that at equal power, the laser pulses contain twice as many photons at a twice longer wavelength). For example, H loss (27 315 cm^{-1}, 326.8 kJ/mol) requires at least 36 photons at 770 cm^{-1} (band A) and 19 photons at 1460 cm^{-1} (band K), whereas for H_2 loss (33 734 cm^{-1}, 403.6 kJ/mol) 44 photons at 770 cm^{-1} and 24 photons at

Downloaded 16 Apr 2010 to 145.18.109.182. Redistribution subject to AIP license or copyright; see http://jcp.aip.org/jcp/copyright.jsp

TABLE IV. Selected structural parameters of azulene and the most stable isomer of protonated azulene (C4-AzuH$^+$) evaluated at the B3LYP/6-311G** level. (Distances of C–C and C–H bonds are given in Ångstrom. C–C–C bond angles are listed in degrees. Δ corresponds to the structural changes upon protonation.)

r_{CC}	Azu	AzuH$^+$	Δ	R_{CH}	Azu	AzuH$^+$	Δ	α_{CCC}	Azu	AzuH$^+$	Δ
r_1	1.3895	1.3821	−0.0074	R_1	1.0879	1.0865	−0.0014	α_1	129.0	128.2	−0.8
r_2	1.3956	1.4035	0.0079	R_2	1.0855	1.0852	−0.0003	α_2	128.7	128.7	0
r_3	1.3953	1.3873	−0.0080	R_3	1.0868	1.0852	−0.0016	α_3	129.9	128.8	−1.1
r_4	1.4040	1.5070	0.1030	R_4	1.0810	1.0984	0.0174	α_4	108.5	103.6	−4.9
r_5	1.4026	1.4925	0.0899	R_5	1.0824	1.0818	−0.0006	α_5	109.9	110.7	0.8
r_6	1.4988	1.4277	−0.0711	R_8	1.0810	1.0814	0.0004	α_6	106.5	107.7	1.2
r_7	1.4040	1.4494	0.0454	R_9	1.0879	1.0859	−0.0020	α_7	106.5	108.3	1.8
r_8	1.4026	1.3508	−0.0518	R_{10}	1.0855	1.0854	−0.0001	α_8	108.5	109.8	1.3
r_9	1.3956	1.3857	−0.0099					α_9	129.0	128.2	−0.8
r_{10}	1.3953	1.4040	0.0087					α_{10}	128.7	129.1	0.4
r_{11}	1.3895	1.4047	−0.0152					α_{11}	127.3	127.9	0.6
								α_{12}	127.3	129.0	1.7

1460 cm^{-1} are needed. The fact that the ratio is independent of the photon energy indicates that the heating rate via IR absorption is fast compared to the fragmentation rate. Finally, it is noted that for protonated benzene elimination of H_2 is calculated to be energetically more favorable than H atom loss,[70] and indeed the only fragmentation channel observed upon IR activation.[27] On the other hand, for H$^+$PAH with more than two rings the loss of atomic hydrogen is the only IRMPD channel detected,[45] indicating that the H_2 loss channel becomes energetically even more demanding for increasing H$^+$PAH size. This observation indicates that the radical cation becomes relatively more stable for the larger PAH molecules.

E. Structures and charge distributions

After the energetics, the impact of protonation at the C4 atom of azulene on the structural parameters is considered by comparing the geometries of Azu and C4-AzuH$^+$ evaluated at the B3LYP/6-311G** level (Fig. 1). Table IV summarizes the salient parameters, namely, the C–C bond lengths (r_i), the C–H bond lengths (R_i), and the C–C–C bond angles (α_i). In agreement with previous high-level calculations[47–49] and spectroscopic evidence,[50–54] azulene is found to have a planar geometry with C_{2v} symmetry and quite regular five- and seven-membered aromatic rings in its $^1A_1$ electronic ground state. All C–C bond lengths are similar (1.3895–1.4040 Å), with the notable exception of the significantly longer C–C bond fusing both rings (r_6=1.4988 Å). This result is consistent with the view that the aromatic stabilization by the 10 π electrons is mainly coming from the conjugating peripherical C–C bonds, whereas the ring fusing bond is essentially a single C–C bond. Similarly, all C–H bonds of Azu are rather similar (1.0810–1.0879 Å), as are the C–C–C bond angles within the five- and also within the seven-membered ring (106.5°–109.9°, 127.3°–129.1°). The deviations of the equilibrium rotational constants (A_e=0.095 246, B_e=0.041 870, C_e=0.029 084 cm^{-1}) from those measured[51,54] for the ground vibrational state (A_0=0.094 797, B_0=0.041 857, C_0=0.028 639 cm^{-1}) are rather small (ΔA=0.5%, ΔB=0.03%, ΔC=1.6%), confirming the suitability of the chosen theoretical level.

As expected, the largest impact of protonation at the C4 atom on the Azu geometry occurs in the five-membered ring. Although the aromatic character of the molecule is removed, the C4-AzuH$^+$ isomer has a planar structure with C_s symmetry in its $^1A'$ electronic ground state (Fig. 1). Only the two H atoms of the methylenic CH_2 group are out of the symmetry plane. As the C4 atom changes from sp^2 to sp^3 hybridization upon protonation, the C6-C4-C5 bond angle α_4 decreases by 5°, whereas all other angles of this ring open up by 0.8°–1.8°. The C–C bond lengths adjacent to the CH_2 group (r_4,r_5) substantially increase by ~0.1 Å. This reduction in bond order through protonation is compensated by a contraction of the adjacent C–C bonds of the five-membered ring by 0.05–0.07 Å (r_6,r_8) and an elongation of the C7-C8 bond (r_7) by 0.05 Å. In contrast, the changes in C–C bonds in the seven-membered ring are minor and below 0.015 Å. The CH_2 bond angle in C4-AzuH$^+$ of 105.7° is typical for sp^3 hybridization, and the aliphatic C–H bond lengths (R_4) are significantly longer than that of Azu (by 0.0174 Å). In contrast, the other C–H bond lengths are nearly unaffected ($|\Delta R_i| < 0.002$ Å). In general, the structural parameters of Azu and C4-AzuH$^+$ obtained at the MP2 level are similar to those at the B3LYP level, with comparable protonation-induced changes. Thus, it is not obvious to extract from the calculated geometries any simple explanation for the failure of the MP2 level to describe the IR spectra of AzuH$^+$.

Analysis of the NBO charge distribution reveals that all H atoms in azulene are uniformly positively charged (+0.20e), whereas the C atoms bear the negative partial charges (q/e=−0.12, −0.23, −0.15, −0.25, −0.17, −0.05, for C1-C6). The dipole moments of 0.4 D (NBO) and 1.0 D (Mulliken), respectively, compare reasonably well with the experimental value of 0.8 D.[50] The excess charge introduced by protonation at the C4 atom is distributed rather uniformly over the whole molecule. The positive partial charge on the aromatic CH protons increases on average from 0.03e to 0.23e, which is slightly lower than on the two aliphatic CH_2 protons (0.27e). The CH_2 group is quite neutral (+0.08e), and the main increase in positive charge is on every alternating C atom by approximately 0.1e (i.e., C2, C6, C5, C7, and C10).

Downloaded 16 Apr 2010 to 145.18.109.182. Redistribution subject to AIP license or copyright; see http://jcp.aip.org/jcp/copyright.jsp

F. Vibrational assignments

The structural changes upon protonation translate directly into modifications of the vibrational properties. Vibrational frequencies and IR intensities of Azu and C4-AzuH$^+$ are listed in Table V, and the calculated and experimental IR spectra of both species are compared in Fig. 6. The experimental IR spectrum of azulene is taken from the NIST database.[66] The 48 normal modes of azulene can be classified in the C_{2v} point group into $17a_1+6a_2+9b_1+16b_2$, and their description can be found in the literature.[47,49,53] Nearly all fundamental frequencies have been measured and assigned by IR and Raman spectroscopy.[53] Good agreement is obtained with the calculated values (Table V), confirming the conclusion that the B3LYP/6-311G** level provides a reliable description of the vibrational properties of this type of molecules. Protonation at the C4 atom reduces the symmetry from C_{2v} to C_s, and introduces three additional normal modes, namely, the antisymmetric aliphatic CH_2 stretch (2944 cm^{-1}), the CH_2 torsion (1120 cm^{-1}), and the CH_2 scissoring motion (1359 cm^{-1}). In total, there are 17 out-of-plane (a″) and 34 in-plane (a′) normal modes of C4-AzuH$^+$. The symmetry reduction and the geometry changes induced by protonation change the composition of the normal modes in terms of their internal displacement vectors. This mixing influences the frequencies and IR intensities and complicates the direct comparison of the vibrational modes of Azu and C4-AzuH$^+$ for certain vibrations, in particular the C–H stretch, C–C stretch, and C–H bend modes with large contributions from atoms of the five-membered ring.

A detailed comparison of the IRMPD spectrum of AzuH$^+$ with the simulated spectrum of C4-AzuH$^+$ is shown in Fig. 7. The gray line in the theoretical spectrum indicates the threshold of 10 km/mol for the IR intensity. Apparently, transitions with IR intensities lower than 10 km/mol are too weak to be observed by IRMPD. This threshold behavior of the IRMPD mechanism arises from the multiple photon absorption process and is well documented in the literature.[37] In the present case, this threshold is rather low, indicating high sensitivity of the experimental approach, which is partly due to a combination of a relatively low dissociation threshold of AzuH$^+$ (327 kJ/mol, 3.4 eV) and the low symmetry of the medium-size molecule, giving rise to fast intramolecular vibrational energy redistribution rates.

Band A of AzuH$^+$ centered at 770 cm^{-1} can readily be assigned to the C–H out-of-plane bending vibration of C4-AzuH$^+$, in which all C atoms vibrate in phase against all H atoms. This isolated and strongly IR active mode is predicted at 775 cm^{-1} with an intensity of 79 km/mol. The corresponding mode of neutral azulene with b_1 symmetry is also strongly IR active and observed at slightly lower frequency (764 cm^{-1}), in good agreement with the theoretical spectrum (757 cm^{-1}, 116 km/mol). The predicted blueshift upon protonation of 18 cm^{-1} is somewhat smaller than the experimental one (6 cm^{-1}), likely due to the 10–20 cm^{-1} redshift induced by the IRMPD mechanism.

The theoretical spectrum of C4-AzuH$^+$ shows a weak transition at 816 cm^{-1} (12 km/mol), corresponding to an in-plane C–C bending mode of the five-membered ring. The

TABLE V. Theoretical frequencies (cm^{-1}) of azulene (C_{2v}) and the most stable isomer of protonated azulene (C4-AzuH$^+$, C_s) evaluated at the B3LYP/6-311G** level are compared to experimental values (Figs. 6 and 7).

	Azu		C4-AzuH$^+$	
	Calc[a]	Exp[b]	Calc[a]	Exp
In-plane	3119 (12, a_1)	3087	3129 (1, a′)	
	3111 (14, b_2)	3076	3112 (2, a′)	
	3093 (7, a_1)	3080	3085 (0, a′)	
	3066 (25, a_1)	3063	3078 (0, a′)	
	3058 (35, b_2)	3058	3070 (0, a′)	
	3039 (7, a_1)	3032	3062 (0, a′)	
	3031 (14, b_2)	3042	3058 (0, a′)	
	3029 (0, a_1)	3022	2921 (9, a′)	
	1591 (3, b_2)	1587	1590 (5, a′)	
	1581 (59, a_1)	1576 (N)	1566 (14, a′)	1577 (N)
	1529 (7, a_1)	1533 (M)	1549 (19, a′)	1555 (M)
	1483 (9, b_2)	1477	1519 (13, a′)	
	1441 (9, b_2)	1454 (K2)	1469 (148, a′)	1461 (L)
	1439 (18, a_1)	1447	1438 (30, a′)	1439 (K2)
	1382 (0, b_2)		1429 (68, a′)	1439 (K1)
			1359 (15, a′)	1353 (H2)
	1375 (91, a_1)	1408 (K1)	1347 (53, a′)	1353 (H1)
	1293 (2, b_2)	1301	1316 (23, a′)	1325 (G)
	1279 (2, b_2)	1288 (F)	1269 (15, a′)	1282 (F)
	1259 (2, a_1)	1264 (D)	1236 (10, a′)	1240 (E2)
	1203 (1, a_1)	1211 (E1)	1227 (7, a′)	1240 (E1)
	1198 (7, b_2)	1204 (E2)	1183 (39, a′)	1182 (D)
	1148 (0, b_2)	1153	1117 (0, a′)	
	1046 (7, a_1)	1054	1095 (9, a′)	
	1030 (1, b_2)	1047	1030 (1, a′)	
	990 (13, b_2)	968 (C)	951 (15, a′)	962 (C)
	930 (2, a_1)	942	934 (0, a′)	
	886 (2, a_1)	899	873 (2, a′)	
	806 (6, a_1)	821 (B)	816 (12, a′)	791 (B)
	720 (0, b_2)	709	722 (4, a′)	
	658 (1, a_1)	675	651 (1, a′)	
	482 (2, b_2)	483	485 (0, a′)	
	398 (1, a_1)	404	394 (0, a′)	
	327 (1, b_2)	333	327 (0, a′)	
Out-of-plane			2944 (1, a″)	
			1120 (1, a″)	
	976 (0, b_1)	968	1032 (0, a″)	
	961 (0, a_2)		1020 (0, a″)	
	944 (5, b_1)	954	980 (3, a″)	
	910 (0, b_1)	899	958 (0, a″)	
	847 (0, a_2)		915 (9, a″)	
	770 (0, a_2)	773	860 (0, a″)	
	757 (116, b_1)	764 (A)	775 (79, a″)	770 (A)
	717 (3, b_1)	759	702 (1, a″)	
	701 (0, a_2)	702	660 (15, a″)	
	592 (1, b_1)	593	558 (1, a″)	
	556 (10, b_1)	558	407 (7, a″)	
	415 (0, a_2)	418	334 (10, a″)	
	310 (11, b_1)	311	285 (2, a″)	
	165 (2, b_1)	181	149 (2, a″)	
	158 (0, a_2)	171	132 (0, a″)	

[a]Calculated at the B3LYP/6-311G** level and scaled by 0.9679. IR intensities (in km/mol) and symmetry species are listed in parentheses.
[b]References 53 and 49.

Downloaded 16 Apr 2010 to 145.18.109.182. Redistribution subject to AIP license or copyright; see http://jcp.aip.org/jcp/copyright.jsp

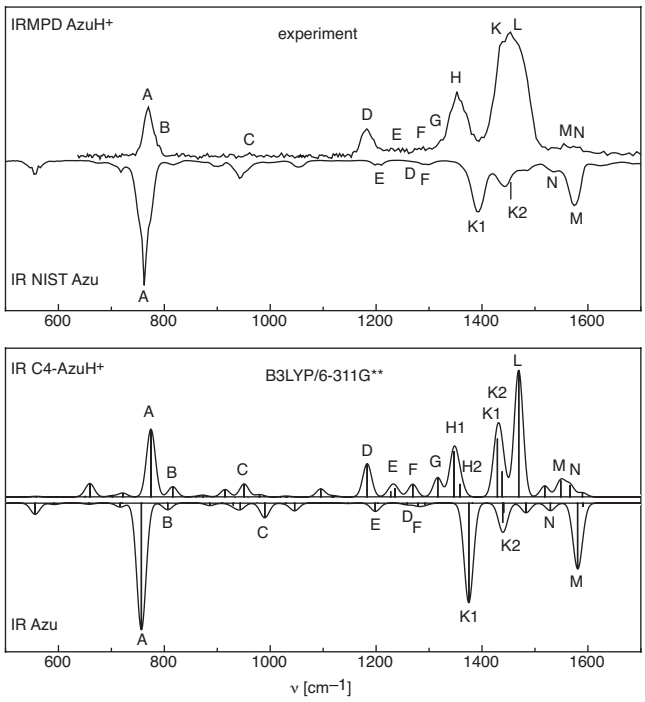

FIG. 6. (Top) IRMPD spectrum of $AzuH^+$ compared to the experimental IR absorption spectrum of azulene (Ref. 66). (bottom) Linear IR absorption spectra of C4-$AzuH^+$ and Azu calculated at the B3LYP/6-311G** level, using a convolution width of 20 cm^{-1} (FWHM) and a scaling factor of 0.9679.

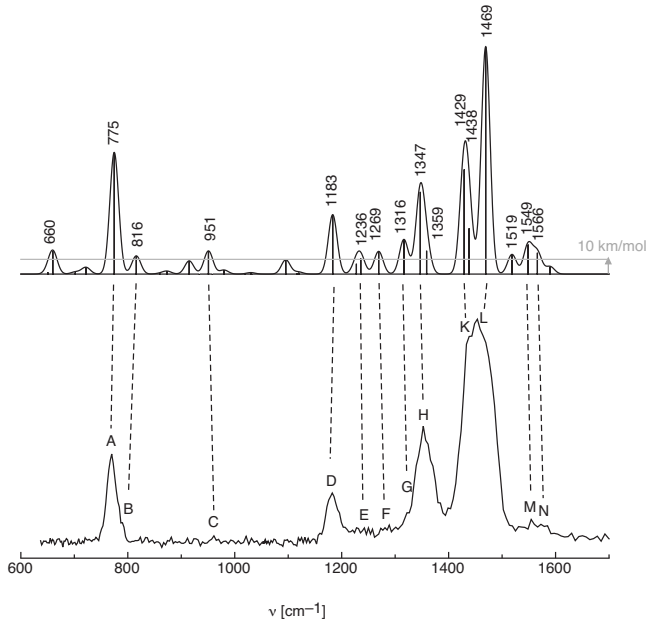

FIG. 7. IRMPD spectrum of $AzuH^+$ (bottom) compared to the linear IR absorption spectrum of the most stable isomer of protonated azulene (C4-$AzuH^+$, top) calculated at the B3LYP/6-311G** level, using a convolution width of 20 cm^{-1} (FWHM) and a scaling factor of 0.9679. The dashed line indicates corresponding transitions. Transitions with a calculated IR intensity larger than 10 km/mol (indicated by the gray line) are listed in cm^{-1}.

IRMPD spectrum displays indeed a weak shoulder of band A at 791 cm^{-1} (B), which is tentatively assigned to this mode. The corresponding fundamental of neutral azulene is predicted at 806 cm^{-1} (a_1) and observed at 821 cm^{-1}. Thus, the predicted protonation-induced shift of −10 cm^{-1} is somewhat smaller than the measured shift of −30 cm^{-1}, which is again attributed to the IRMPD mechanism.

The tentative detection of band C at 962 cm^{-1} in the IRMPD spectrum correlates with the weakly IR active mode of C4-$AzuH^+$ (15 km/mol) predicted as an isolated transition at 951 cm^{-1}. This mode has significant stretching character of the C4-C5 bond (r_5), which is elongated upon protonation. Thus, the frequency of this mode is significantly redshifted from the corresponding vibration of neutral Azu predicted at 990 cm^{-1} (b_2, 13 km/mol) and observed at 968 cm^{-1}.

Band D centered at 1182 cm^{-1} in the IRMPD spectrum is assigned to the isolated fundamental predicted at 1183 cm^{-1} (39 km/mol) of C4-$AzuH^+$. This in-plane mode involves C–H bending and C7-C8 and C4-C6 stretch character (r_7,r_4). As both C–C bonds substantially elongate upon protonation, the corresponding mode of neutral Azu occurs at much higher frequency (1259 cm^{-1}, a_1). However, as its IR intensity is rather low, this mode is hardly visible in the IR spectrum of the neutral molecule. The predicted protonation-induced redshift of 76 cm^{-1} is consistent with the measured one of 82 cm^{-1}.

The weak and somewhat broader band E at 1240 cm^{-1} in the IRMPD spectrum is attributed to two overlapping transitions of C4-$AzuH^+$ predicted at 1227 and 1239 cm^{-1}, with intensities of 7 and 10 km/mol, respectively. The 1227 cm^{-1} (denoted E1) corresponds to an in-plane C–H bend localized at the seven-membered ring, whereas the 1239 cm^{-1} mode (denoted E2) is a C–H bend of both rings, in particularly involving also the CH_2 group. In the neutral molecule, both modes with a_1 and b_2 symmetries are predicted at significantly lower frequency (1203 and 1198 cm^{-1}), in agreement with the experimental observations (1211 and 1204 cm^{-1}).

Band F at 1282 cm^{-1} in the IRMPD spectrum is assigned to an isolated transition of C4-$AzuH^+$ calculated at 1269 cm^{-1} (15 km/mol). This mode is again mainly an in-plane C–H bend localized on the seven-membered ring, and is thus hardly shifted from the corresponding transition of neutral azulene predicted at 1279 cm^{-1} (2 km/mol, b_2) and observed at 1288 cm^{-1}.

Band G in the IRMPD spectrum identified at around 1325 cm^{-1} in the shoulder of the intense band H is attributed to the predicted transition at 1316 cm^{-1} (23 km/mol) of C4-$AzuH^+$. This mode is described by C–H bending with contribution of the CH_2 group. Due to mode mixing, it is difficult to correlate this vibration with a corresponding normal mode of the neutral molecule.

The intense and somewhat broader band H with a maximum at 1353 cm^{-1} the IRMPD spectrum arises from two overlapping fundamental transitions of C4-$AzuH^+$, namely, the intense C–H bend (denoted H1) localized on the five-membered ring predicted at 1347 cm^{-1} (53 km/mol) and the approximately three times weaker CH_2 scissoring mode at 1359 cm^{-1} (15 km/mol) denoted H2. The corresponding neutral C–H bend is predicted at slightly higher frequency (1382 cm^{-1}, b_2) and is experimentally not observed due to vanishing IR activity. The scissoring mode of C4-$AzuH^+$ is unique to the protonated molecule. Hence, the intense band H of the IRMPD spectrum of C4-$AzuH^+$ has no corresponding transition in the IR spectrum of Azu.

Downloaded 16 Apr 2010 to 145.18.109.182. Redistribution subject to AIP license or copyright; see http://jcp.aip.org/jcp/copyright.jsp

The next intense transition in the convoluted IR spectrum calculated for C4-AzuH$^+$ is band K, which is composed of two overlapping transitions at 1429 and 1438 cm^{-1} (denoted K1 and K2) with large and medium IR intensities of 68 and 30 km/mol, respectively. Experimentally, both transitions are observed in the IRMPD spectrum as a single unresolved shoulder at 1439 cm^{-1} occurring in the low-frequency wing of the intense band L. The more intense 1429 cm^{-1} band (K1) corresponds largely to the C6-C7 stretch. As the strength of this bond (r_6) increases drastically upon protonation, the corresponding mode of neutral Azu is calculated at much lower frequency at 1375 cm^{-1} and also with high IR intensity. The experimental frequency shift of this mode upon protonation, $1439-1408=31$ cm^{-1}, compares favorably with the theoretical shift, $1429-1375=54$ cm^{-1}, when taking the 10–20 cm^{-1} redshift of the IRMPD mechanism into account. The weaker theoretical 1438 cm^{-1} component (K2) is mainly an in-plane bend of the seven-membered ring and thus not shifted much by protonation from the corresponding neutral value (1441 cm^{-1}, 9 km/mol, b_2). Again, the experimental frequency shift of this mode upon protonation, $1439-1454=-15$ cm^{-1}, compares favorably with the theoretical shift, $1438-1441=-3$ cm^{-1}, when including the 10–20 cm^{-1} redshift of the IRMPD mechanism.

The most intense band in the IRMPD spectrum (L) occurs with its maximum at 1461 cm^{-1} and is assigned to an isolated transition of C4-AzuH$^+$ calculated at 1469 cm^{-1} (148 km/mol). Due to a strong change in character of this coupled C–C stretch mode upon protonation, it is difficult to identify a corresponding normal mode in the neutral molecule. Significantly, there is no mode with comparable IR intensity in the calculated and experimental IR spectrum of Azu.

The weak band M at 1555 cm^{-1} in the IRMPD spectrum is attributed to the calculated transition of C4-AzuH$^+$ at 1549 cm^{-1} (19 km/mol), corresponding to a coupled C–C stretch fundamental. The analogous mode in neutral Azu is predicted at 1581 cm^{-1} with higher IR intensity (59 km/mol) and observed at 1576 cm^{-1}. Thus, the measured redshift upon protonation of 21 cm^{-1} is compatible with the predicted shift of 32 cm^{-1}.

The highest-frequency transition detected in the IRMPD spectrum, band N at 1577 cm^{-1}, has its theoretical counterpart at 1566 cm^{-1} (14 km/mol), which is again a coupled C–C stretch mode. The corresponding neutral frequency is calculated as 1529 cm^{-1} (7 km/mol) and measured as 1533 cm^{-1}. The measured protonation-induced blueshift of 44 cm^{-1} is consistent with the predicted value of 37 cm^{-1}.

In general, the protonation has quite significant effects on the vibrational IR spectrum, both on the frequencies and IR intensities (Fig. 6). The calculations at the B3LYP level reproduce these IR spectra and the protonation-induced changes well and enable the assignment of all experimental features. In total, 15 vibrations of C4-AzuH$^+$ could be identified in the IRMPD spectrum, with an average deviation of 9 cm^{-1} between measured and calculated frequencies (Table V).

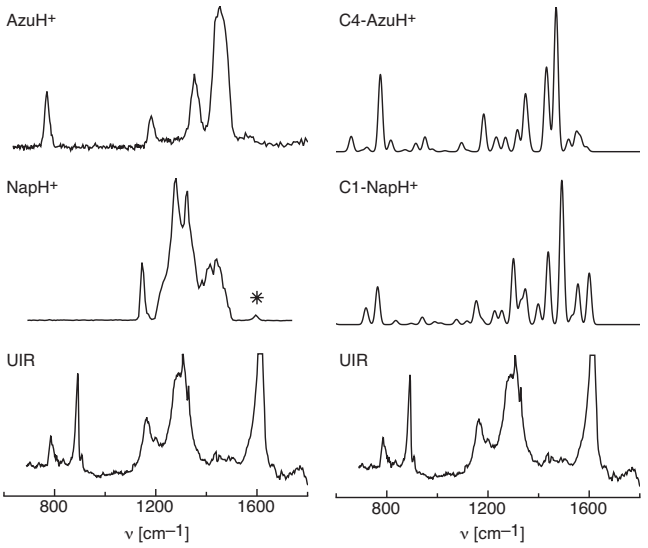

FIG. 8. IRMPD spectra of protonated azulene (AzuH$^+$) and naphthalene (NapH$^+$) (Ref. 35) are compared to linear IR absorption spectra of C4-AzuH$^+$ and C1-NapH$^+$ calculated at the B3LYP/6-311G** level. For comparison, the UIR spectrum representative of a highly ionized region (Orion Bar) is shown as well (Ref. 5). The asterisk marks a transition, for which the IRMPD efficiency was lowered probably due to atmospheric water absorption in the FEL beam path.

G. Comparison with protonated naphthalene and the UIR spectrum

In Fig. 8 the IRMPD spectra of AzuH$^+$ and protonated naphthalene (NapH$^+$) (Ref. 35) are compared with linear IR absorption spectra of C4-AzuH$^+$ and C1-NapH$^+$ calculated at the B3LYP/6-311G** level. The IRMPD spectrum of NapH$^+$ was recorded previously with the IR-FEL at CLIO, whereby the ions were produced by chemical ionization. The conditions were such that only bands with intensities larger than 50 km/mol could be detected, which explains the absence of any transition below 1100 cm^{-1} in the IRMPD spectrum.[35] Moreover, the laser power dropped significantly above 1400 cm^{-1} so that the predicted intense 1600 cm^{-1} band was observed only weakly in the experiment. Attempts to record the IRMPD spectrum of NapH$^+$ under the present experimental conditions at FELIX failed due to low ion currents generated in the ESI source. The latter observation is rationalized by the low proton affinity of naphthalene (802.9 kJ/mol), which is considerably lower than that of NH_3 (PA=853.6).[57] As can be seen in Fig. 8, the calculated IR spectra of both $C_{10}H_9^+$ isomers are quite different and this result is largely confirmed by the experimental IRMPD spectra.

Figure 8 compares also the IR spectra of AzuH$^+$ and NapH$^+$ with an astronomical UIR spectrum representative of a highly ionized region of the interstellar medium. The UIR spectrum chosen originates from the Orion Bar region in the M42 nebula and was recorded with the short wavelength spectrometer onboard the Infrared Space Observatory satellite.[5] As mentioned in the Introduction, there are reasonable chemical arguments for predicting protonated PAH molecules in this environment[4] and in highly ionized regions of the interstellar medium in general. H$^+$PAH molecules can be efficiently generated by protonation of PAH or by H atom

Downloaded 16 Apr 2010 to 145.18.109.182. Redistribution subject to AIP license or copyright; see http://jcp.aip.org/jcp/copyright.jsp

attachment to PAH^+. Once formed, H^+PAH molecules are found to be quite unreactive toward both H and H_2.[4] Although most chemical models predict PAH molecules in the size range of 20–80 C atoms to be (photo-)chemically most stable,[5] there have been claims that the naphthalene cation has been identified in the interstellar medium via its electronic spectrum.[72]

The UIR bands are emission bands of vibrationally hot species. Thus, the vibrational transitions observed are shifted in frequency from the frequencies of fundamental transitions due to vibrational anharmonicities. Similarly, the multiple-photon nature of the IRMPD process also shifts the frequencies to lower values in comparison with fundamental transitions, again via the effect of anharmonicities. Thus, it is indeed meaningful to compare IRMPD spectra with the UIR bands, as both processes and the resulting IR spectra are affected by the same type of vibrational anharmonicity.[38] As was noted previously,[35] the IRMPD spectrum of $NapH^+$ shows indeed good agreement with the UIR spectrum when taking into account the deficiencies of the experimental spectrum described above. This conclusion is supported by a very recent report of the IR spectrum of cold $NapH^+-Ar$ complexes.[73] For $AzuH^+$, the agreement is much less favorable, indicating that the $AzuH^+$ is not a major carrier of the UIR spectrum. This conclusion is not surprising, as naphthalene is calculated to be more stable than isomeric azulene by 145 kJ/mol, and thermal isomerization from azulene to naphthalene has been observed under elevated temperatures.

IV. CONCLUSIONS

In the present work, protonated azulene has been characterized by IR spectroscopy and quantum chemical calculations. The IRMPD spectrum of $AzuH^+$ was obtained in the informative fingerprint range by coupling an ESI-FTICR with the IR-FEL FELIX. Significantly, this IR spectrum corresponds to the first spectroscopic detection of this fundamental carbocation. The potential energy surface of $AzuH^+$ has been investigated for the first time in some detail at the B3LYP/6-311G** and CBS-QB3 levels, providing energies of global and local minima, barriers for isomerization, dissociation energies, and proton affinities. The observed IRMPD spectrum was obtained in the H (80%) and H_2 (20%) loss channels, which correspond to the two lowest energy fragment channels with calculated appearance energies of 327 and 404 kJ/mol, respectively. Comparison with IR spectra of all six conceivable $AzuH^+$ isomers calculated at the B3LYP level demonstrates unambiguously that protonation occurs predominantly at the C4 atom of Azu, which is by far the most stable isomer ($by > 80$ kJ/mol). No clear sign of the less stable isomers is observed. Interestingly, the MP2 level fails to predict reliable IR spectra even when relatively large basis sets (up to 6-311+G**) are employed. In general, protonation has a profound impact on the geometry of azulene and, as a consequence, quite significant effects on the vibrational IR spectrum, both on the frequencies and the IR intensities. Calculations at the B3LYP level reproduce the protonation-induced changes well and enable the assignment of all experimental transitions observed in the IRMPD spectrum. In total, 15 vibrations of C4-$AzuH^+$ are identified and assigned, with an average deviation of less than 10 cm^{-1} between measured and calculated frequencies. Comparison of the IRMPD spectrum of $AzuH^+$ with that of protonated naphthalene ($NapH^+$) shows that both isomers can be clearly distinguished by their IR spectra in the fingerprint range. Whereas the IRMPD spectrum of $NapH^+$ reveals good agreement with the astronomical UIR spectrum characteristic for highly ionized regions of the interstellar medium, the agreement with the IRMPD spectrum of $AzuH^+$ is less favorable. Clearly, IRMPD spectra of larger H^+PAH are required to further test and confirm the hypothesis that these species are present in interstellar space. Indeed, first IRMPD spectra of protonated coronene support this proposition.[45]

ACKNOWLEDGMENTS

This work was supported by the Fonds der Chemischen Industrie, the Deutsche Forschungsgemeinschaft (Grant No. DO 729/3). We acknowledge support by the European Community-Research Infrastructure Action under the FP6 "Structuring the European Research Area Program" (through the integrated infrastructure initiative "Integrating Activity on Synchrotron and Free Electron Laser Science"). We also acknowledge excellent support from the FELIX team (B. Redlich, A. F. G. van der Meer, and G. Berden).

[1] F. A. Carey and R. J. Sundberg, *Advanced Organic Chemistry* (Plenum, New York, 1995); M. B. Smith and J. March, *Advanced Organic Chemistry: Reactions, Mechanisms, and Structure*, 5th ed. (Wiley, New York, 2001); G. A. Olah, Acc. Chem. Res. **4**, 240 (1971).
[2] V. A. Koptyug, Top. Curr. Chem. **122**, 1 (1984); V. B. Mochalin and Y. N. Porshnev, Russ. Chem. Rev. **46**, 530 (1977).
[3] P. Weilmünster, A. Keller, and K. H. Homann, Combust. Flame **116**, 62 (1999).
[4] T. Snow, L. V. Page, Y. Keheyan, and V. M. Bierbaum, Nature (London) **391**, 259 (1998).
[5] A. Tielens, Annu. Rev. Astron. Astrophys. **46**, 289 (2008).
[6] *The Physics and Chemistry of the Interstellar Medium*, edited by A. G. G. M. Tielens (Cambridge University Press, London, 2005).
[7] O. V. Boyarkin, S. R. Mercier, A. Kamariotis, and T. R. Rizzo, J. Am. Chem. Soc. **128**, 2816 (2006); H. Kang, C. Dedonder-Lardeux, C. Jouvet, G. Gregoire, C. Desfrancois, J. P. Schermann, M. Barat, and J. A. Fayeton, J. Phys. Chem. A **109**, 2417 (2005).
[8] D. H. Aue, M. Guidoni, and L. D. Betowski, Int. J. Mass Spectrom. **201**, 283 (2000).
[9] S. Fornarini, Mass Spectrom. Rev. **15**, 365 (1996); S. Fornarini and M. E. Crestoni, Acc. Chem. Res. **31**, 827 (1998); D. Kuck, Mass Spectrom. Rev. **9**, 583 (1990).
[10] B. S. Freiser and J. L. Beauchamp, J. Am. Chem. Soc. **98**, 3136 (1976); **99**, 3214 (1977).
[11] N. Solcà and O. Dopfer, J. Am. Chem. Soc. **125**, 1421 (2003).
[12] N. Solcà and O. Dopfer, Chem. Phys. Lett. **342**, 191 (2001).
[13] O. Dopfer, J. Phys. Org. Chem. **19**, 540 (2006).
[14] M. Okumura, L. I. Yeh, and Y. T. Lee, J. Chem. Phys. **83**, 3705 (1985); J. M. Lisy, *ibid.* **125**, 132302 (2006); A. L. Nicely, D. J. Miller, and J. M. Lisy, J. Am. Chem. Soc. **131**, 6314 (2009); A. Fujii, E. Fujimaki, T. Ebata, and N. Mikami, J. Chem. Phys. **112**, 6275 (2000); M. A. Duncan, Int. J. Mass Spectrom. **200**, 545 (2000); J. R. Roscioli, L. R. McCunn, and M. A. Johnson, Science **316**, 249 (2007); E. J. Bieske and O. Dopfer, Chem. Rev. (Washington, D.C.) **100**, 3963 (2000); O. Dopfer, D. Roth, and J. P. Maier, J. Am. Chem. Soc. **124**, 494 (2002); H. S. Andrei, S. A. Nizkorodov, and O. Dopfer, Angew. Chem. **119**, 4838 (2007); H. S. Andrei, N. Solca, and O. Dopfer, Angew. Chem., Int. Ed. **47**, 395 (2008).
[15] N. Solcà and O. Dopfer, Angew. Chem., Int. Ed. **41**, 3628 (2002).
[16] N. Solcà and O. Dopfer, Chem. Eur. J. **9**, 3154 (2003).
[17] G. E. Douberly, A. M. Ricks, P. V. R. Schleyer, and M. A. Duncan, J. Phys. Chem. A **112**, 4869 (2008).

Downloaded 16 Apr 2010 to 145.18.109.182. Redistribution subject to AIP license or copyright; see http://jcp.aip.org/jcp/copyright.jsp

[18] C. Chaudhuri, C.-C. Wu, J.-C. Jiang, and H.-C. Chang, Aust. J. Chem. **57**, 1153 (2004).
[19] N. Solcà and O. Dopfer, J. Am. Chem. Soc. **126**, 1716 (2004); J. Chem. Phys. **120**, 10470 (2004).
[20] N. Solcà and O. Dopfer, Angew. Chem., Int. Ed. **42**, 1537 (2003).
[21] N. Solcà and O. Dopfer, ChemPhysChem **6**, 434 (2005).
[22] F. Pasker, N. Solcà, and O. Dopfer, J. Phys. Chem. A **110**, 12793 (2006).
[23] H. S. Andrei, N. Solcà, and O. Dopfer, ChemPhysChem **7**, 107 (2006).
[24] J. A. Stearns, S. Mercier, C. Seaiby, M. Guidi, O. V. Boyarkin, and T. R. Rizzo, J. Am. Chem. Soc. **129**, 11814 (2007); J. A. Stearns, O. V. Boyarkin, and T. R. Rizzo, *ibid.* **129**, 13820 (2007); J. A. Stearns, M. Guidi, O. V. Boyarkin, and T. R. Rizzo, J. Chem. Phys. **127**, 154322 (2007); T. D. Vaden, T. de Boer, J. P. Simons, and L. C. Snoek, Phys. Chem. Chem. Phys. **10**, 1443 (2008).
[25] N. A. Macleod and J. P. Simons, Mol. Phys. **104**, 3317 (2006).
[26] N. Solcà and O. Dopfer, J. Chem. Phys. **121**, 769 (2004).
[27] W. Jones, P. Boissel, B. Chiavarino, M. E. Crestoni, S. Fornarini, J. Lemaire, and P. Maitre, Angew. Chem., Int. Ed. **42**, 2057 (2003).
[28] O. Dopfer, N. Solcà, J. Lemaire, P. Maitre, M. E. Crestoni, and S. Fornarini, J. Phys. Chem. A **109**, 7881 (2005).
[29] B. Chiavarino, M. E. Crestoni, S. Fornarini, J. Lemaire, L. MacAleese, and P. Maitre, ChemPhysChem **6**, 437 (2005).
[30] O. Dopfer, J. Lemaire, P. Maitre, M. E. Crestoni, and S. Fornarini, Int. J. Mass Spectrom. **249–250**, 149 (2006).
[31] B. Chiavarino, M. E. Crestoni, S. Fornarini, O. Dopfer, J. Lemaire, and P. Maitre, J. Phys. Chem. A **110**, 9352 (2006).
[32] U. J. Lorenz, J. Lemaire, P. Maitre, M.-E. Crestoni, S. Fornarini, and O. Dopfer, Int. J. Mass Spectrom. **267**, 43 (2007).
[33] J. Oomens, G. Meijer, and G. von Helden, Int. J. Mass Spectrom. **249–250**, 199 (2006).
[34] J. Oomens, G. von Helden, and G. Meijer, J. Phys. Chem. A **108**, 8273 (2004).
[35] U. J. Lorenz, N. Solca, J. Lemaire, P. Maitre, and O. Dopfer, Angew. Chem., Int. Ed. **46**, 6714 (2007).
[36] J. Y. Salpin, S. Guillaumont, J. Tortajada, L. MacAleese, J. Lemaire, and P. Maitre, ChemPhysChem **8**, 2235 (2007).
[37] J. Oomens, B. G. Sartakov, G. Meijer, and G. von Helden, Int. J. Mass Spectrom. **254**, 1 (2006).
[38] J. Oomens, A. G. G. M. Tielens, B. G. Sartakov, G. von Helden, and G. Meijer, Astrophys. J. **591**, 968 (2003).
[39] L. MacAleese and P. Maitre, Mass Spectrom. Rev. **26**, 583 (2007); T. D. Fridgen, *ibid.* **28**, 586 (2009); J. R. Eyler, *ibid.* **28**, 448 (2009); N. C. Polfer and J. Oomens, *ibid.* **28**, 468 (2009); R. H. Wu and T. B. McMahon, *ibid.* **28**, 546 (2009).
[40] A. Leger and J. L. Puget, Astron. Astrophys. **137**, L5 (1984); L. J. Allamandola, A. G. G. M. Tielens, and J. R. Barker, Astrophys. J. **290**, L25 (1985).
[41] *The Diffuse Interstellar Bands*, edited by A. G. G. M. Tielens and T. P. Snow (Kluwer Academic, London, 1995); G. H. Herbig, Annu. Rev. Astron. Astrophys. **33**, 19 (1995); P. Jenniskens and F. X. Desert, Astrophys. J. Suppl. Ser. **106**, 39 (1994).
[42] E. Peeters, S. Hony, C. Van Kerckhoven, A. Tielens, L. J. Allamandola, D. M. Hudgins, and C. W. Bauschlicher, Astron. Astrophys. **390**, 1089 (2002); S. Schlemmer, D. J. Cook, J. A. Harrison, B. Wurfel, W. Chapman, and R. J. Saykally, Science **265**, 1686 (1994).
[43] M. Hammonds, A. Pathak, and P. J. Sarre, Phys. Chem. Chem. Phys. **11**, 4458 (2009); A. Pathak and P. J. Sarre, Mon. Not. R. Astron. Soc. **391**, L10 (2008).
[44] V. Le Page, T. P. Snow, and V. M. Bierbaum, Astrophys. J. **584**, 316 (2003).
[45] H. Knorke, J. Langer, J. Oomens, and O. Dopfer, Astrophys. J. **706**, L66 (2009).
[46] L. J. Allamandola, A. G. G. M. Tielens, and J. R. Barker, Astrophys. J., Suppl. Ser. **71**, 733 (1989).
[47] P. M. Kozlowski, G. Rauhut, and P. Pulay, J. Chem. Phys. **103**, 5650 (1995).
[48] J. M. L. Martin, J. ElYazal, and J. P. Francois, J. Phys. Chem. **100**, 15358 (1996); A. Murakami, T. Kobayashi, A. Goldberg, and S. Nakamura, J. Chem. Phys. **120**, 1245 (2004).
[49] S. J. Mole, X. Zhou, J. G. Wardeska, and R. Liu, Spectrochim. Acta, Part A **52**, 1211 (1996).
[50] H. J. Tobler, A. Bauder, and H. H. Gunthard, J. Mol. Spectrosc. **18**, 239 (1965).
[51] S. Huber, G. Grassi, and A. Bauder, Mol. Phys. **103**, 1395 (2005).
[52] S. Thorwirth, P. Theule, C. A. Gottlieb, M. C. McCarthy, and P. Thaddeus, Astrophys. J. **662**, 1309 (2007).
[53] A. Bree, A. J. Pal, and C. Taliani, Spectrochim. Acta, Part A **46**, 1767 (1990).
[54] Y. Semba, K. Yoshida, S. Kasahara, C. K. Ni, Y. C. Hsu, S. H. Lin, Y. Ohshima, and M. Baba, J. Chem. Phys. **131**, 024303 (2009).
[55] M. Meot-Ner, J. Phys. Chem. **84**, 2716 (1980).
[56] M. Meot-Ner (Mautner), Int. J. Mass Spectrom. **227**, 525 (2003).
[57] E. P. L. Hunter and S. G. Lias, J. Phys. Chem. Ref. Data **27**, 413 (1998).
[58] M. V. Frash, A. C. Hopkinson, and D. K. Bohme, J. Am. Chem. Soc. **123**, 6687 (2001).
[59] J. J. Valle, J. R. Eyler, J. Oomens, D. T. Moore, A. F. G. van der Meer, G. von Helden, G. Meijer, C. L. Hendrickson, A. G. Marshall, and G. T. Blakney, Rev. Sci. Instrum. **76**, 023103 (2005); D. Oepts, A. F. G. van der Meer, and P. W. van Amersfoort, Infrared Phys. Technol. **36**, 297 (1995).
[60] M. J. Frisch, G. W. Trucks, H. B. Schlegel, *et al.*, GAUSSIAN 03, Revision C.02., Gaussian, Inc, Pittsburgh PA, 2004.
[61] J. A. Montgomery, M. J. Frisch, J. W. Ochterski, and G. A. Petersson, J. Chem. Phys. **110**, 2822 (1999).
[62] M. P. Andersson and P. Uvdal, J. Phys. Chem. A **109**, 2937 (2005).
[63] D. K. Malick, G. A. Petersson, and J. A. Montgomery, J. Chem. Phys. **108**, 5704 (1998).
[64] D. Heidrich, Angew. Chem., Int. Ed. **41**, 3208 (2002).
[65] K. Pointet, A. Milliet, S. Hoyau, and M. F. RenouGonnord, J. Comput. Chem. **18**, 629 (1997).
[66] P. J. Linstrom and W. G. Mallard, *NIST Chemistry WebBook* (NIST Standards and Technology, Gaithersburg, 2001).
[67] NIST Computational Chemistry Comparison and Benchmark Database, NIST Standards and Technology, Gaithersburg MD, 2006.
[68] C. W. Bauschlicher, Jr., Astrophys. J. **509**, L125 (1998).
[69] D. Ascenzi, D. Bassi, P. Franceschi, O. Hadjar, P. Tosi, M. Di Stefano, M. Rosi, and A. Sgamellotti, J. Chem. Phys. **121**, 6728 (2004).
[70] E. del Rio, R. Lopez, and T. L. Sordo, J. Phys. Chem. A **101**, 10090 (1997).
[71] O. Dopfer, R. V. Olkhov, and J. P. Maier, J. Chem. Phys. **111**, 10754 (1999).
[72] S. Iglesias-Groth, A. Manchado, D. A. Garcia-Hernandez, J. I. G. Hernandez, and D. L. Lambert, Astrophys. J. **685**, L55 (2008).
[73] A. M. Ricks, G. E. Douberly, and M. A. Duncan, Astrophys. J. **702**, 301 (2009).

Downloaded 16 Apr 2010 to 145.18.109.182. Redistribution subject to AIP license or copyright; see http://jcp.aip.org/jcp/copyright.jsp